DOI: http://dx.doi.org/10.15407/techned2018.01.023

ELECTRIC FIELD DURING TRANSIENT PROCESS OF CONFIGURATION CHANGING OF WATER MICRO-INCLUSIONS IN LIQUID DIELECTRICS

M.A. Shcherba*
Institute of Electrodynamics National Academy of Sciences of Ukraine,
pr. Peremohy, 56, Kyiv, 03057, Ukraine, e-mail: m.shcherba@gmail.com

Mathematical modeling and analysis of the distribution of the electric field near closely located water microinclusions in a liquid dielectric under the transitional process of changing their shape and mutual arrangement are performed. With continuous deformation, convergence and fusion of microinclusions, a dynamic problem was solved to determine their shape and relative position at each instant of time under the action of electrical and mechanical forces. The dependence of the rates of deformation, approach and merging of inclusions (which determine the duration of the transient process upon reaching the equilibrium form of the resulting inclusion) is investigated from the initial distance of the inclusions and on the strength of the external electric field. References 16, figures 5.
Key words: electric field, water microinclusions, liquid dielectric, dynamic problem, mathematical modeling, transient process, equilibrium form.

Introduction. The appearance of conductive microinclusions or other heterogeneous microdefects in dielectric media disturbs the external electric field (EF), increasing its intensity near the poles of these defects along the field [4, 5, 13]. The disturbed EF accelerates the processes of degradation of dielectrics, and in some cases, in particular, when the dielectric strength of the material is exceeded, it can cause the electric breakdown of this dielectrics [4, 14]. In practice, the configuration (shape and relative location) of microinclusions can vary with time under the action of external forces [10]. The solution of such a class of dynamic problems is quite complex, since it requires the large computational resources and the application not only spatial discretization, but additionally temporal one [9, 15]. The development of modern numerical methods for calculating multi-physical processes and their software implementations makes it possible to solve the problems unsolvable earlier [3, 7].

One of this problems is the calculation of EF in the dielectrics near water microinclusions when their configuration changes. In the external field, under the action of dielectrophoresis forces, the water molecules can move in the region of the greatest intensity of the EF, combining into joint conducting structures [3, 16]. As an example of typical demonstration of this mechanism is appearance and development of water trees (thin branched structures) in cables with cross-linked polyethylene (XLPE) insulation [4, 8].

Modern practical problems require the calculation of EF disturbances in solid, liquid and gaseous dielectrics (for example, near water trees in XLPE insulation, near water droplets in transformer oil or water droplets in the air near power line wires). If the configuration of the inclusions in a solid dielectric is determined by the presence of micro-pores and micro-cracks in the material [4, 6], then in the liquid and gaseous media the shape and mutual arrangement of the inclusions can rapidly change, since the dynamic mechanisms limited only the forces of interphase tension or surface one will be demonstrated much more [1].

At present, numerical methods, in particular the finite element method, are widely used to solve problems of calculation of inhomogeneous EF distribution. This method allows to take into account the real geometry of the analyzed elements in the computational domain and the materials properties that are often nonlinear [7]. According to this approach, a boundary-value problem is solved for a limited computational domain with given conditions (Dirichlet or Neumann) on its boundaries and the boundaries of various media within the region.

The main distinction of dynamic problems is the changing form of these boundaries, which must be calculated and taken into account in the algorithm for solving differential equations. There are several approaches to working with changing boundaries, such as the level set method [9], the phase field method [15] and its variation for the three-component immiscible liquids – ternary phase field method [15]. In particular, in this paper we used the phase field method, which more accurately reflects the physical processes in the problem being solved.

*ORCID ID: http://orcid.org/0000-0001-6616-4567

An important class of problems is the calculation of the nonuniform EF distribution in a liquid dielectric, the various types of which are widely used in the elements of equipment for electro-energy purposes. There are known works on calculating the field near microinclusions of the equilibrium configuration [4, 10, 13], but little attention has been paid to the study of EF amplifications during the transient processes. During the transient processes there will be micro-defect configurations that can disturb the field stronger; therefore, this work was devoted to the analysis of such disturbances.

The aim of the work was the development of a mathematical model and the solution of the dynamic problem of calculating the distribution of the electric field near closely located water microinclusions in a liquid dielectric under the transient process of their deformation, convergence and fusion.

Physico-mathematical formulation of the problem. The EF distribution was calculated in a liquid dielectric (by the example of transformer oil) with water microinclusions. The problem under consideration is a multi-physical problem [3], consisting of interrelated electrical and hydrodynamic subtasks with varying boundaries.

Electrical subtask. It was simulated the region of the dielectric of the cylindrical shape (for the use of an axially symmetric description) with such dimensions that there were not edge effects on its boundaries (height 500 μm, diameter 300 μm), see Fig. 1. A constant voltage of 200–300 V or a sinusoidal voltage with an effective value of 200–300 V with a frequency of 50 Hz was applied to the cylinder. In other words, the average intensity of the EF is E_{av} = 0.4–0.6 kV/mm, which is a characteristic value for the transformer oil.

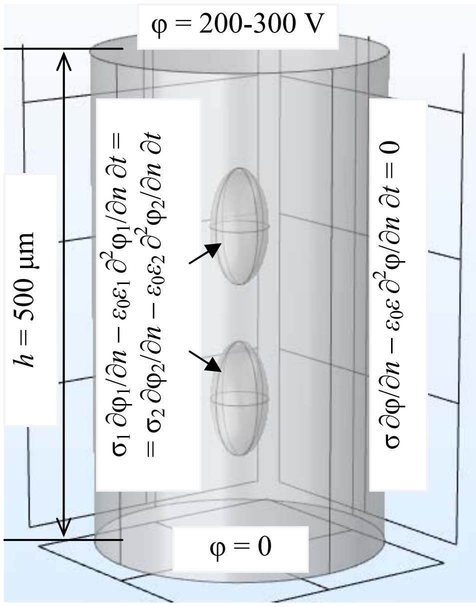

Fig. 1

The presence of a single or two closely located microinclusions of the most characteristic forms (spheres and ellipsoids of rotation with different semi-axes) and with volumes of each 65 417 μm^3, which corresponds to a spherical microinclusion with a radius of 25 μm, was considered in the insulator.

The media were considered as homogeneous, isotropic and linear one. The problem was described in a quasi-static approximation by the system of Maxwell's equations [2]. The calculated equation for the scalar electric potential φ as in [4, 11, 12] was written as:

$$\operatorname{div}\left(\sigma \operatorname{grad}\varphi - \varepsilon\varepsilon_0 \frac{\partial \operatorname{grad}\varphi}{\partial t}\right) = 0, \tag{1}$$

where σ, ε – the electrical conductivity and dielectric permittivity of the media.

Equation (1) at the upper and lower boundaries of the computational domain, shown in Fig. 1, was supplemented by the Dirichlet conditions, i.e. by setting the values of the potentials φ. On the lateral faces of the computational domain, it was supplemented by the Neumann conditions, i.e. equality to zero the derivatives of the potentials along the normal to the surface ***n***, which corresponds to the absence of currents in these directions. At the interface dielectric–microinclusion, the conditions for the equality of the scalar potentials and their derivatives along the normal to the surface were set [4, 11, 12]:

$$\varphi_1 = \varphi_2, \qquad \sigma_1\, \partial\varphi_1/\partial n - \varepsilon_0\varepsilon_1\, \partial^2\varphi_1/\partial n\, \partial t = \sigma_2\, \partial\varphi_2/\partial n - \varepsilon_0\varepsilon_2\, \partial^2\varphi_2/\partial n\, \partial t, \tag{2}$$

i.e. equality the normal components of the total current density $\boldsymbol{n}\cdot(\boldsymbol{J}_{tot\,1} - \boldsymbol{J}_{tot\,2}) = 0$.

The problem was solved using the finite element method in the COMSOL Multiphysics software package [7], were the distribution of the scalar potential φ was found in the computational domain, divided by the finite element grid.

Under the action of external EF the surface charges are induced at the interface conductor – dielectric and in order to calculate the electric forces $\boldsymbol{f}_S$ acting on them the Maxwell stress tensors $\boldsymbol{T}_{em1}$ and $\boldsymbol{T}_{em2}$, written in the form of the tensor (dyadic) product of the vectors ***E*** and ***D*** [2], are used:

$$\boldsymbol{f}_S = \boldsymbol{n}\cdot(\boldsymbol{T}_{em2} - \boldsymbol{T}_{em1}) = \boldsymbol{n}\cdot(\boldsymbol{E}\otimes\boldsymbol{D}) = \boldsymbol{n}\cdot\varepsilon\varepsilon_0[\boldsymbol{E}\boldsymbol{E}^T - (0{,}5\boldsymbol{E}\cdot\boldsymbol{E})\boldsymbol{I}], \tag{3}$$

where ***I*** is the identity matrix of 3x3.

To take into account the electric forces in the hydrodynamic sub-problem with varying interphase we pass from the surface forces $\boldsymbol{f}_S$ to the volume forces $\boldsymbol{f}_V$. For this purpose, an interphase boundary was considered with finite thickness δ that equals to half the size of the maximum grid element in the region, through which this boundary passes. Within the interface, volume forces $\boldsymbol{f}_V$ were calculated in the form $\boldsymbol{f}_V = \mathrm{div}\boldsymbol{T}_{em}$.

The hydrodynamic subtask. The dielectrophoresis forces under the field strengths under consideration lead to smooth changes in the velocities and pressures of the liquids, so their flow was considered to be laminar and described by the Navier-Stokes equation [1, 7] in the form:

$$\frac{\partial \boldsymbol{v}}{\partial t} = -(\boldsymbol{v}\cdot\nabla)\boldsymbol{v} + \frac{1}{\rho}\mathrm{div}[\boldsymbol{T}_{mech} + \boldsymbol{T}_{em}], \tag{4}$$

$$\boldsymbol{T}_{mech} = -p\boldsymbol{I} + \mu[\mathrm{grad}\boldsymbol{v} + (\mathrm{grad}\boldsymbol{v})^{\mathrm{T}}], \tag{5}$$

where $\boldsymbol{v}$ is the velocities field vector, $\boldsymbol{T}_{mech}$ is the mechanical stress tensor, which is determined according to equation (5), ∇ is the nabla operator, ρ, μ is the density and the kinematic viscosity coefficient of medium, and ρ is the pressure.

The liquid was considered incompressible and equation (4) was supplemented with equation (6):

$$\mathrm{div}\,\boldsymbol{v} = 0. \tag{6}$$

Equations (4) and (6) were supplemented with the Dirichlet condition $\boldsymbol{v} = 0$ at the boundary of the computational domain, and the volumetric electric forces $\boldsymbol{f}_V$, found from the solution of the electric subtask, were taken into account in equation (6) as $\mathrm{div}\boldsymbol{T}_{em}$.

To trace the interphase boundary between liquids, the phase field method (PFM) was used, according to which the boundary conditions at the interface were replaced by a differential equation in partial derivatives for the evolution of some auxiliary field (phase field) described by the variable ϕ [15]. This phase field takes the values +1 for one fluid and –1 for the other one, with a gradual change of values around the interphase boundary, which then diffuses with a finite width. The discrete position of the interphase boundary at a given time is defined as the set of all points where the phase field takes the value $\phi = 1 + (-1) = 0$ (Fig. 2) [15].

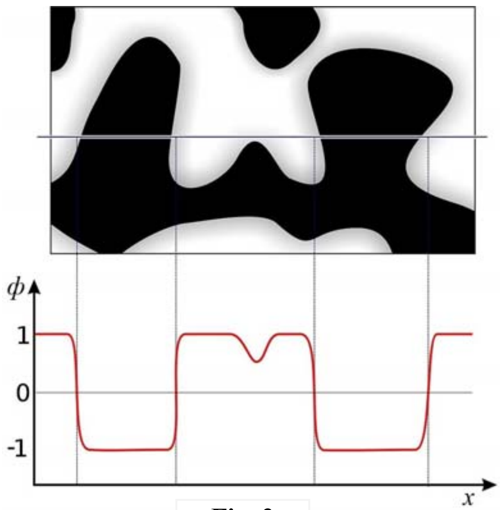

Fig. 2

The interfacial tension force was calculated as the product of the chemical potential G and the gradient of the phase field variable ϕ and was taken into account in the Navier-Stokes equation (4) as part of the volume force $\boldsymbol{f}_V$. The change in the variable ϕ was described by the Kahn-Hilliard equation, which according to the PFM splits into two partial differential equations of the second order in partial derivatives [15]:

$$\frac{\partial \phi}{\partial t} = -\boldsymbol{v}\cdot\mathrm{grad}\phi + \mathrm{div}\left(\frac{\gamma\lambda}{\delta^2}\mathrm{grad}\psi\right), \tag{7}$$

$$\psi = -\mathrm{div}(\delta^2\mathrm{grad}\phi) + (\phi^2 - 1)\phi + \frac{1}{\lambda}\frac{\partial f}{\partial \phi}, \tag{8}$$

where δ is the thickness of the interphase layer, γ – the mobility variable in $m^3 \cdot s/kg$, using which the relaxation time of the transient process is determined, f, λ – the free energy density and stirring energy density.

On the boundary of the computational domain, equations (7) and (8) were supplemented with the following conditions:

$$\boldsymbol{n}\cdot\frac{\gamma\lambda}{\delta^2}\mathrm{grad}\psi = 0, \qquad \boldsymbol{n}\cdot\mathrm{grad}\varphi = \cos(\theta)\left|\mathrm{grad}\varphi\right|, \tag{9}$$

where $\boldsymbol{n}$ is the normal vector to the surface, and θ – the wetting angle.

Results of the numerical experiment. The distribution of the electric field near the closely located water microinclusions in the liquid dielectric (transformer oil) was calculated during the transient process of their continuous deformation, convergence and fusion. The values of EF intensity E were given in relative units in the form of the electric field amplification factor $k_E = E/E_{av}$, i.e. E is referred to the average intensity E_{av} in a dielectric at a distance from microinclusions [4].

The deformation of the spherical and ellipsoidal microinclusions to the equilibrium shape, depending on the ratio of their semi-axes and the magnitude of the intensity of the external EF was calculated to verify the mathematical model (see Fig. 3). The equilibrium shape is achieved when the electric force is balanced by the interfacial tension force. The results obtained on the mathematical model were compared with known analytical solutions for the spherical and ellipsoidal forms of microinclusions [1, 2].

Fig. 3, *a* shows the transient process of the deformation of a spherical microinclusion to the shape of an ellipsoid of revolution in the event of the appearance of a constant EF with intensity E_{av} = 0.55 kV/mm, and Fig. 3, *b* shows the process of inverse deformation to spherical shape in the case of disappearance of the external field. The interface of two liquids is shown by light strip, and a thin dark line in Fig. 3, *b* shows the initial form of the ellipsoidal microinclusion. The intensity of the EF is determined according to the color of the tinting on the scale in Fig. 3 on the right.

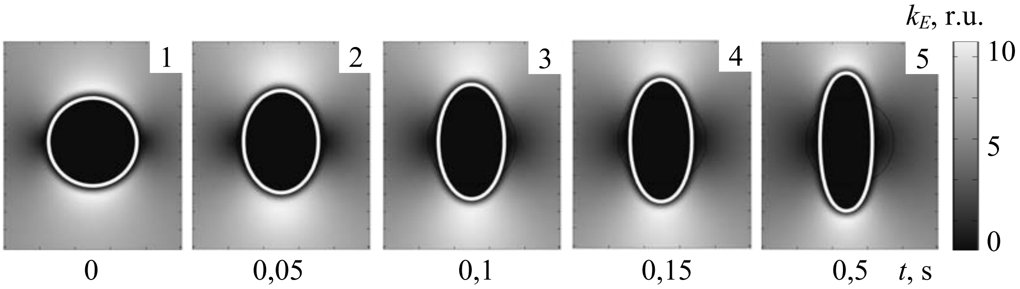

a

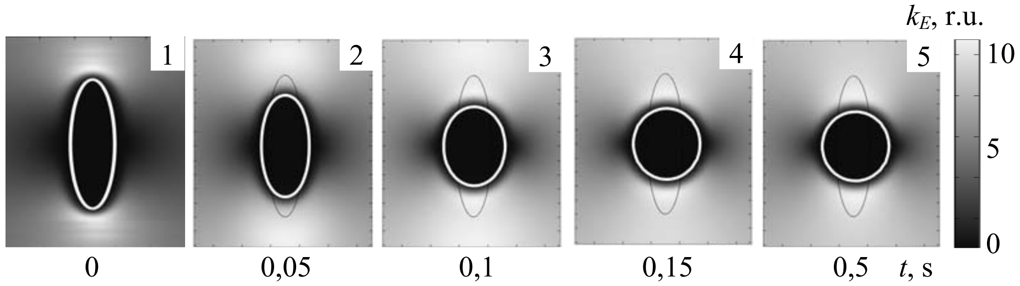

b

Fig. 3

The field amplification factor k_E varied from 3 for the sphere (which coincides with the analytic solution [2]) to 10 for an elongated ellipsoid (which agrees with the results of [4]). Duration each transient processes $t_{t.p.}$ was 0.5 s. Since the alternating EF with a frequency of 50 Hz has a period of 0.02 s, the change in the external field will be manifested in additional regular deformations of the surface of microinclusions with small amplitude.

For two closely spaced microinclusions, at mutual distances of 50, 25, 10, and 5 μm, transient processes were investigated in the event of an external constant and sinusoidal EF with intensity 0.40; 0.45; 0.50; 0.55 and 0.60 kV/mm. Fig. 4, *a* and Fig. 4, *b* show the deformation, convergence and fusion of two closely located spherical microinclusions with diameters of 50 μm at mutual distances of 5 μm and 50 μm at E_{av} = 0.50 kV/mm.

At a distance of 5 μm, the duration of the transient process was 0.3 s, while increasing the distance to 50 μm the duration increased to 2.2 s. The field amplification factor k_E is determined according to the scale in Fig. 4 on the right and it reached the maximum values more than 30 in the dielectric gap between close located microinclusions (slide 1 in Fig. 4, *a* and slide 4 in Fig. 4, *b*). When the microinclusions come in contact, the maximum values of k_E at the external poles of the inclusions take the values k_E = 12 (slide 2 in Fig. 4, *a*) and k_E = 18 (slide 5 in Fig. 4, *b*). As the microinclusions deform to the ellipsoidal form and, correspondingly, their size decreases along the field, the value of k_E decreases to 8 (slide 5 in Fig. 4, *a* and slide 7 in Fig. 4, *b*).

Under the influence of an external field, spherical microinclusions deform to an ellipsoid of revolution, the ratio of the semi-axes of which is determined by the field strength *E*. At the investigated EF intensities, the rate of deformation of single inclusions to the ellipsoid is higher than the rate of their convergence.

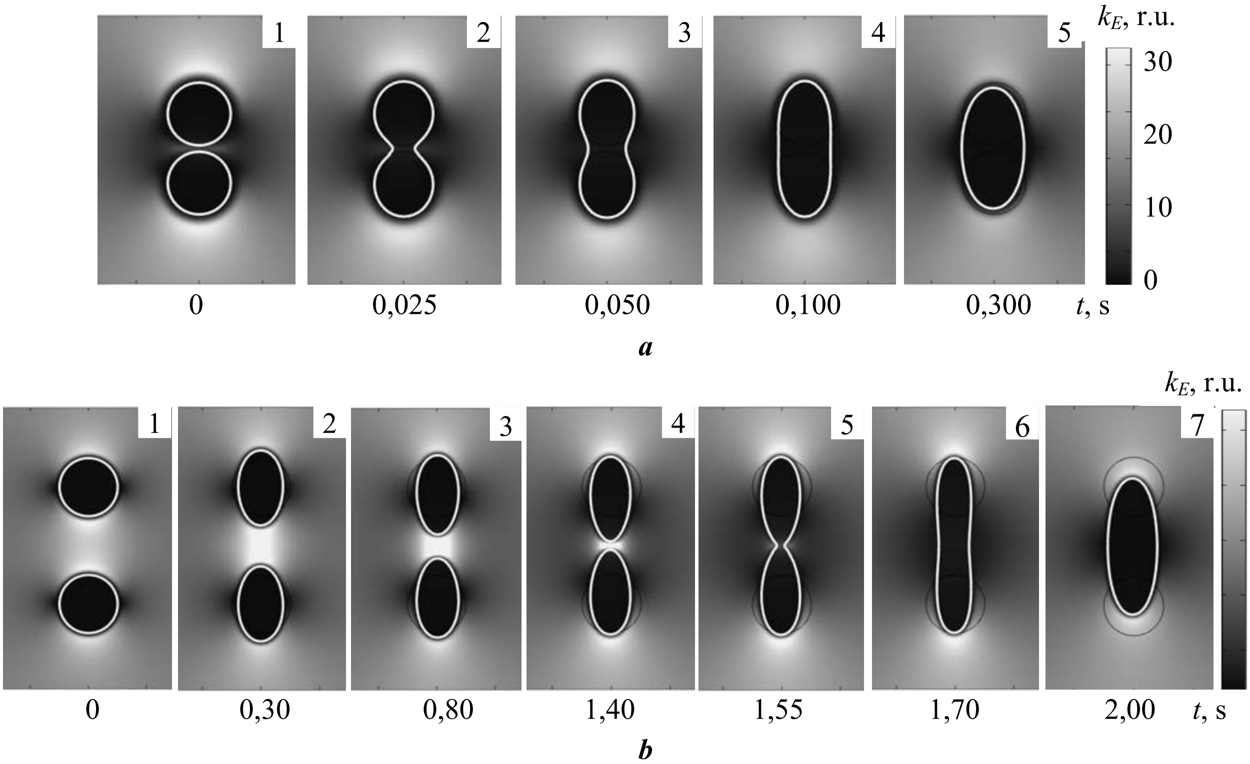

Fig. 4

If the time required for deformation is 0.5 c, then the convergence (determined by dielectrophoresis forces) can last a few seconds (as, for example, in Fig. 4, *b*). In its turn, the fusion of microinclusions after its contact occurs within 0.3–0.5 s.

It should be noted that at close mutual distances (smaller than the size of the inclusions) due to the interaction of the induced surface charges, the microinclusion poles are mutually attracted along the field, additionally deformed, and the shape of the inclusions from the ellipsoidal goes to the "pear-shaped" (slide 4 in Fig. 4, *b*). After the contact, the resultant micro-inclusion takes the form of a dumbbell (slide 2 in Fig. 4, *a* and slide 5 in Fig. 4, *b*), which are deformed to an equilibrium ellipsoidal form (slide 5 in Fig. 4, *a* and slide 7 in Fig. 4, *b*).

The dependence of the duration of the transient process $t_{t.p.}$ on the intensity of the external EF E_{av} was also investigated. Dependences of the duration of the transient process $t_{t.p.}$ on the initial distance between the microinclusions *l* and the intensity of the external EF E_{av} are shown in the graphs in Fig. 5.

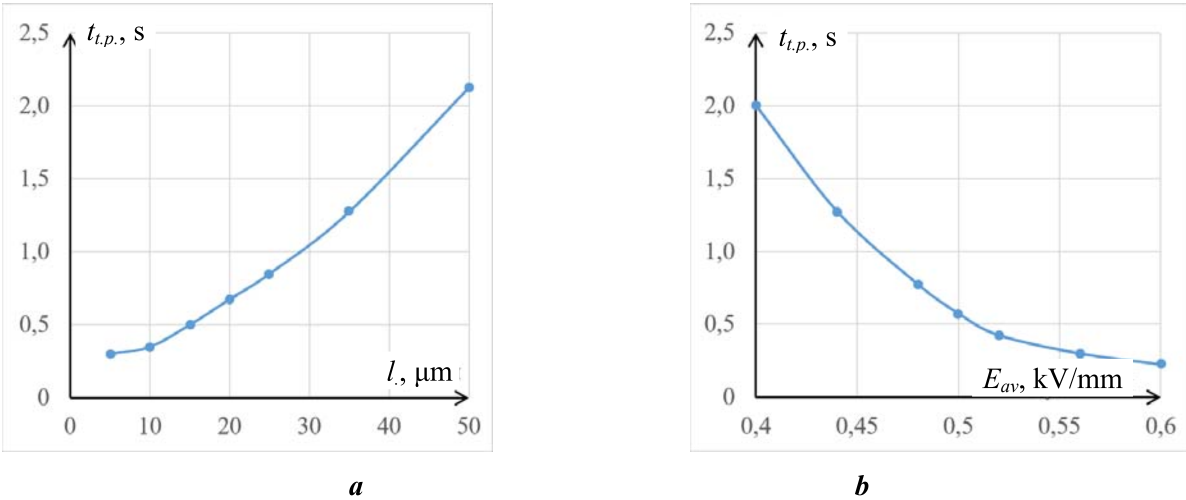

Fig. 5

The numerical experiments have shown that the duration of the transient process increases with increasing distance between microinclusions and decreases with increasing external electric field intensity according to nonlinear dependences. During the convergence of inclusions in the gap between them the EF intensity increases and the factor k_E at extra close distances can reach values of 100, that is more than 30 times greater than $k_E = 3$ for a spherical inclusion. In this case, the region of the stressed volume of the dielectric (the region of increased values of EF, the size of which characterizes the stochastic mechanisms of insulation breakdown) around the inclusions grows.

After the contact, the resultant inclusion takes the form of a dumbbell, for which the EF intensity $k_E = 18$ and is 6 times higher than the value of k_E for a sphere. At the same time, the stressed volume of the dielectric continues to increase, assuming its maximum value at the moment of contact of the inclusions. Thus, during the transient process there are larger field intensifications near the deformed microinclusions than near inclusions of an equilibrium ellipsoidal shape, i.e. configurations during the transient process are more dangerous from the point of view of the occurrence of local breakdowns.

Conclusions.

A three-dimensional mathematical model is developed and an analysis of the distribution of the electric field near closely located water microinclusions in liquid dielectric (transformer oil) during the transient process of their continuous deformation, convergence and fusion under the action of electrical and mechanical forces is performed. The calculation method is based on the numerical finite element method and the phase field method implemented in the Comsol Multiphysics application package. Based on the results of a numerical experiment, it is shown that the duration of the transient process, when microinclusions reach the equilibrium configuration, increases nonlinearly with increasing distance between microinclusions and decreases nonlinearly with increasing external electric field intensity. It has also been demonstrated that microinclusions are deformed faster than attracted under the action of dielectrophoresis forces.

At close mutual distances due to the interaction of induced surface charges, the poles of the inclusions are further deformed, mutually attracting along the field and the shape of the inclusions change from the ellipsoidal form to the "pear-shaped" one. After contact, the resultant inclusion takes the form of a dumbbell, which gradually deforms to an ellipsoidal one with an equilibrium semi-axis relationship. It is shown that the field amplification in a dielectric near such inclusions is greater than near the inclusions of the equilibrium ellipsoidal form, i.e. such configurations during the transient process are more dangerous from the point of view of the occurrence of local breakdowns.

1. *Landau L.D., Lifshyts E.M.* Hydrodynamics, Theor. Physics, vol. VI. Moskva: Fizmatlit, 2016. 736 p. (Rus)

2. *Landau L.D., Lifshyts E.M.* Electrodynamics of continuums, Theor. Physics, vol. VIII. Moskva: Fizmatlit, 2003. 632 p. (Rus)

3. *Podoltsev A.D., Kucheriava I.M.* Multiphysics modeling in electrical engineering. Kiev: Institut Elektrodinamiki Natsionalnoi Akademii Nauk Ukrainy, 2015. 305 p. (Rus)

4. *Shydlovskii A.K., Shcherba A.A., Podoltsev A.D., Kucheriava I.M.* Cables with polymeric insulation on ultrahigh voltage. Kiev: Institut Elektrodinamiki Natsionalnoi Akademii Nauk Ukrainy, 2013. 352 p. (Rus)

5. *Shcherba M.A., Podoltsev A.D.* Electric field and current density distribution near water inclusions of polymer insulation of high-voltage cables in view of its nonlinear properties. *Tekhnichna Elektrodynamika*. 2016. No 1. Pp. 11–19. (Rus)

6. *Burkes K.W., Makram E.B., Hadidi R.* Water Tree Detection in Underground Cables Using Time Domain Reflectometry. IEEE *Power and Energy Technology Systems Journal*. 2015. Vol. 2(2). Pp. 53–62.

7. *Comsol Multiphysics*, https: //www.comsol.com/., Comsol Inc., Burlington, MA, USA, 2017.

8. *Kurihara T., Okamoto T., Kim M.H.* Measurement of residual charge using pulse voltages for water tree degraded XLPE cables diagnosis. IEEE *Trans. on DEI*. 2014. No 21(1). Pp. 321–330.

9. *Olsson E., Kreiss G.* A Conservative Level Set Method for Two Phase Flow. *J. Comput. Phys*. 2005. Vol. 210. Pp. 225–246.

10. *Saniyyati C.N., Arief Y.Z., Ahmad M.H., Piah M.A.M.* Investigation on propensity difference of water tree occurrences in polymeric insulating materials. IEEE Intern. Conf. on *Power Engineering and Optimization*, Langkawi Island (Malaysia). March, 2014. Pp. 413–417.

11. *Shcherba M.A.* Multiphysical processes during electric field disturbance in solid dielectric near water micro-inclusions connected by conductive channels. IEEE Intern. Conf. on *Intelligent Energy and Power Systems*, Kyiv (Ukraine). June, 2016. – Pp. 1–5.

12. *Shcherba M.A., Zolotarev V.M., Belyanin R.V.* The comparison of electric field perturbations by water inclusions in linear and nonlinear XLPE insulation. IEEE Intern. Conf. on *Computational Problems of Electrical Engineering*, Lviv (Ukraine). September, 2015. Pp. 188–191.

13. *Tao W., Song S., Zhang Y., Hao W.* Study on the electric-field characteristics of water tree region on the dry or wet condition in XLPE cables. IEEE Intern. Conf. on *High Voltage Engineering and Application*, Chengdu (China). September, 2016. Pp. 15–18.

14. *Wang W., Tao W., Ma Z., Liu J.* The mechanism of water tree growth in XLPE cables based on the finite element method. IEEE Intern. Conf. on *High Voltage Engineering and Application*, Chengdu (China). September, 2016. Pp. 1–4.

15. *Yue P., Zhou C., Feng J.J., Ollivier-Gooch C.F., Hu H.H.* Phase-field Simulations of Interfacial Dynamics in Viscoelastic Fluids Using Finite Elements with Adaptive Meshing. *J. Comp. Phys*. 2006. Vol. 219. Pp. 47–67.

16. *Zhou K., Li K., Yang M., Huang M.* Insight into the influence of mechanical orientation on water tree propagation according to abnormal water tree shapes. IEEE Intern. Conf. In *Dielectrics, Montpellier* (France). July 2016. Vol. 2. Pp. 836–839.

УДК 621.365.5

ЕЛЕКТРИЧНЕ ПОЛЕ ПРИ ПЕРЕХІДНОМУ ПРОЦЕСІ ЗМІНИ КОНФІГУРАЦІЇ ВОДНИХ МІКРОВКЛЮЧЕНЬ У РІДКИХ ДІЕЛЕКТРИКАХ

М.А. Щерба, канд.техн.наук
Інститут електродинаміки НАН України,
пр. Перемоги, 56, Київ, 03057, Україна,
e-mail: m.shcherba@gmail.com

Виконано математичне моделювання та аналіз розподілу електричного поля біля близько розташованих водних мікровключень у рідкому діелектрику при перехідному процесі зміни їх форми і взаємного розташування. При неперервній деформації, зближенні і злитті мікровключень вирішувалася динамічна задача по визначенню їхньої форми і взаємного розташування в кожний момент часу при дії електричних і механічних сил. Досліджено залежність швидкостей деформації, зближення і злиття включень (які визначають тривалість перехідного процесу до досягнення рівноважної форми результуючого включення) від початкової віддаленості включень і від напруженості зовнішнього електричного поля. Бібл. 16, рис. 5.

Ключові слова: електричне поле, водні мікровключення, рідкий діелектрик, динамічна задача, математичне моделювання, перехідний процес, рівноважна форма.

УДК 621.365.5

ЭЛЕКТРИЧЕСКОЕ ПОЛЕ ПРИ ПЕРЕХОДНОМ ПРОЦЕССЕ ИЗМЕНЕНИЯ КОНФИГУРАЦИИ ВОДНЫХ МИКРОВКЛЮЧЕНИЙ В ЖИДКИХ ДИЭЛЕКТРИКАХ

М.А. Щерба, канд.техн.наук
Институт электродинамики НАН Украины,
пр. Победы, 56, Киев, 03057, Украина,
e-mail: m.shcherba@gmail.com

Выполнено математическое моделирование и анализ распределения электрического поля возле близко расположенных водных микровключений в жидком диэлектрике при переходном процессе изменения их формы и взаимного расположения. При непрерывной деформации, сближении и слиянии микровключений решалась динамическая задача по определению их формы и взаимного расположения в каждый момент времени при действии электрических и механических сил. Исследована зависимость скоростей деформации, сближения и слияния включений (которые определяют длительность переходного процесса по достижению равновесной формы результирующего включения) от начальной удаленности включений и от напряженности внешнего электрического поля. Библ. 16, рис. 5.

Ключевые слова: электрическое поле, водные микровключения, жидкий диэлектрик, динамическая задача, математическое моделирование, переходный процесс, равновесная форма.

Надійшла 11.09.2017
Остаточний 19.09.2017